

Understanding the pharmacokinetics of prodrug and metabolite

Seungil Cho and Young-Ran Yoon

Molecular Diagnostics and Imaging Center, School of Medicine, Kyungpook National University; Clinical Trial Center, Kyungpook National University Hospital, Daegu 41944, Korea

*Correspondence: S. Cho; Tel: +82-53-200-6358, Fax: +82-53-422-4950, E-mail: chosi1@gmail.com

Y-R. Yoon; Tel: +82-53-420-4950, Fax: +82-53-426-4944, E-mail: yry@knu.ac.kr



Keywords

Pharmacokinetics,
Prodrug,
Formation rate-limited,
Elimination rate-limited,
Metabolism

pISSN: 2289-0882

eISSN: 2383-5427

This tutorial explains the pharmacokinetics of a prodrug and its active metabolite (or parent drug) using a two-step, consecutive, first-order irreversible reaction as a basic model for prodrug metabolism. In this model, the prodrug is metabolized and produces the parent drug, which is subsequently eliminated. The mathematical expressions for pharmacokinetic parameters were derived step by step. In addition, we visualized these expressions to help understand the relationship between pharmacokinetic parameters easily. For the elimination rate-limited and formation rate-limited metabolism, we analyzed the plasma drug concentration versus time curve of a prodrug administered intravenously.

Introduction

Prodrug is a pharmacologically inactive derivative of an active drug and undergoes in vivo biotransformation to release the active drug by chemical or enzymatic cleavages.[1-3] A prodrug strategy is typically used when a pharmacologically active drug has poor solubility or permeability.[1,2] Various chemically or enzymatically labile functional groups have been introduced to improve the properties of the parent drug and decrease the pre-systemic metabolism.[1,2] Many successful examples have been reviewed in the literature.[1-3] A detailed discussion of prodrugs and their active metabolites (parent drugs) is beyond the scope of this tutorial. Here we focus on the pharmacokinetics of a prodrug and its metabolite to help understand their pharmacokinetic data obtained from preclinical and clinical studies. This will ultimately help define the proper dose of the prodrug needed for efficacy.

Theoretical Analysis

Prodrug Kinetics

When a prodrug is administered orally, it undergoes complicated processes of absorption, distribution, metabolism, and excretion. To understand these processes for metabolites, Cummings and Martin published results on the excretion and accrual of drug metabolites in 1963.[4] This provides the basis for the pharmacokinetics of drug and its metabolites and can be readily applied to study the pharmacokinetics of prodrug. Since then, many theoretical analyses and reviews, related to prodrug pharmacokinetics, have been published.[5-10] A thorough understanding of prodrug kinetics is daunting and may be achieved using sophisticated physiologically based pharmacokinetic (PBPK) modeling.[11,12]

To get some insight pertinent to prodrug kinetics, we consider a simple scheme for the fate of a prodrug (P) after intravenous administration (Fig. 1). A fraction of the prodrug (f) is metabolized and produces a parent drug (D) with a first-order formation rate constant, $k_{f(D)}$. The drug (D) may be further metabolized to a daughter metabolite (DM_1) or excreted. The elimination rate constant of the parent drug, $k_{el(D)}$, is expressed by the sum of the formation rate constant of the daughter metabolite, $k_{f(DM1)}$, and the urinary excretion rate constant, $k_{ex(D)}$. More than one metabolite may be formed with a formation rate constant, $k_{f(PM2)}$, and then excreted with a rate constant, $k_{ex(PM2)}$. Otherwise, a fraction of the drug is excreted into urine as unchanged form (P) with a rate constant, $k_{ex(P)}$. The overall

Copyright © 2018 Seungil Cho and Young-Ran Yoon
© It is identical to the Creative Commons Attribution Non-Commercial License (<http://creativecommons.org/licenses/by-nc/3.0/>).
© This paper meets the requirement of KS X ISO 9706, ISO 9706-1994 and ANSI/NISO Z.39.48-1992 (Permanence of Paper).

Reviewer

This article was invited and reviewed by the editors of TCP.

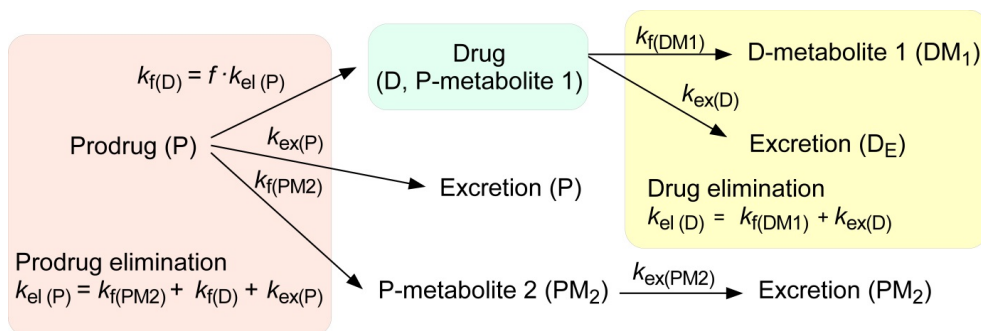
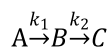


Figure 1. A model to describe the kinetics of a prodrug and its metabolites. The prodrug (P) is metabolized or excreted unchanged according to the elimination rate constant ($k_{el(P)}$). The drug (D) is eliminated according to the elimination rate constant ($k_{el(D)}$). See text for details.

elimination rate constant of the prodrug, $k_{el(P)}$, is the sum of $k_{f(D)}$, $k_{f(PM2)}$, and $k_{ex(P)}$. No matter how complex the pathways may appear, the time course for the change of metabolite amount can be described by a general relationship: rate of change of metabolite amount in body = rate of formation – rate of elimination. [5,6] However, a full mathematical description of this model is still complex and difficult to solve. We will further simplify this model to have clear understanding of the factors influencing the amount of parent drug in the body.

A basic model for prodrug kinetics

Consider a simple case of a two-step consecutive first-order irreversible reaction:



This model provides the basis for developing more complex models. Thus it is crucial to understand this reaction kinetics thoroughly for further study. Here, we use simple notations for the sake of clarity. We can set up the following three differential equations to describe the change in amounts of A, B, and C over time.

$$\frac{dA}{dt} = -k_1 A \quad (1)$$

$$\frac{dB}{dt} = k_1 A - k_2 B \quad (2)$$

$$\frac{dC}{dt} = k_2 B \quad (3)$$

At $t = 0$, $A = A_0$ and $B = C = 0$, and $A + B + C = A_0$ at all times. The Eq. (1) can be solved immediately to give

$$A = A_0 e^{-k_1 t} \quad (4)$$

Substituting Eq. (4) into Eq. (2), we get

$$\frac{dB}{dt} + k_2 B = k_1 A_0 e^{-k_1 t} \quad (5)$$

Eq. (5) can be solved simply by noting that

$$\frac{d}{dt}(B e^{k_2 t}) = \left(\frac{dB}{dt} + k_2 B \right) e^{k_2 t}$$

By multiplying both sides of Eq. (5) by $e^{k_2 t}$ and using the above relationship, we get

$$d(B e^{k_2 t}) = k_1 A_0 e^{(k_2 - k_1)t} dt \quad (6)$$

If $k_1 \neq k_2$, integration of Eq. (6) from $t = 0$ to t gives

$$B = \frac{k_1 A_0}{k_2 - k_1} (e^{-k_1 t} - e^{-k_2 t}) \quad (7)$$

In the special case when $k_1 = k_2$, Eq. (6) can reduce to

$$d(B e^{k_1 t}) = k_1 A_0 dt.$$

Then, the integrated expression becomes

$$B = k_1 A_0 t e^{-k_1 t}. \quad (8)$$

The expression for C can be obtained using the mass balance relationship, $C = A_0 - A - B$,

$$C = \frac{A_0}{k_2 - k_1} ((k_2 - k_1) + k_1 e^{-k_2 t} - k_2 e^{-k_1 t}). \quad (9)$$

Figure 2 shows a typical amount-time profile of each species for the consecutive **first-order irreversible reaction**. The amount of A decreases at the normal exponential rate characteristic of a first-order decay curve (blue line). The amount of B follows a bi-exponential profile, first rising and then declining (red line). The amount of C continuously increases and reaches a plateau (green line). This profile is useful for quantifying absorption and elimination processes of drug as well as formation and elimination processes of metabolite. [13,14]

To calculate the maximum amount of B (B_{max}) and the time to reach the peak (t_{max}), we take the derivative of Eq. (7), set the derivative, dB/dt , to zero, and rearrange to obtain

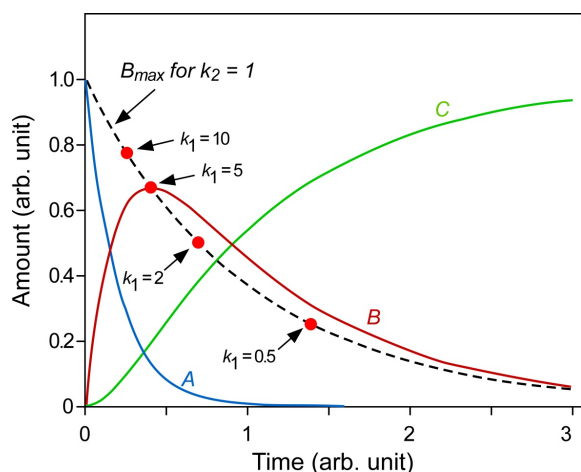


Figure 2. Amount-time profile for a two-step irreversible consecutive first-order reaction: $A \xrightarrow{k_1} B \xrightarrow{k_2} C$. The abscissa and ordinate represent time and amount of each species, respectively, in arbitrary units. The case illustrated was simulated using Microsoft Excel for $k_1 = 5$, $k_2 = 1$, and $A_0 = 1$. The B_{\max} curve (dashed line) was obtained using Eqns. (11), (13), and (14) for $k_2 = 1$. The dots represent B_{\max} for given values of k_1 . See text for details.

$$\frac{k_2}{k_1} = \frac{e^{-k_1 t_{\max}}}{e^{-k_2 t_{\max}}} \quad (10)$$

Take the natural logarithm of both sides and solve for t_{\max} to get

$$t_{\max} = \frac{1}{k_2 - k_1} \ln \frac{k_2}{k_1} \quad (11)$$

The resulting B_{\max} at t_{\max} then becomes

$$B_{\max} = \frac{k_1 A_0}{k_2 - k_1} (e^{-k_1 t_{\max}} - e^{-k_2 t_{\max}}) \quad (12)$$

Using Eq. (10), we obtain

$$B_{\max} = A_0 e^{-k_2 t_{\max}} \quad (13)$$

From Eq. (11), we get

$$-k_2 t_{\max} = \frac{k_2}{k_2 - k_1} \ln \frac{k_1}{k_2}$$

Therefore,

$$B_{\max} = A_0 \left(\frac{k_1}{k_2} \right)^{\frac{k_2}{k_2 - k_1}} \quad (14)$$

In Figure 2, we also visualized the Equations (11), (13), and (14) to show that t_{\max} decreases and B_{\max} increases as the ratio of k_1 to k_2 increases (dashed line). In other words, when k_2 is smaller than k_1 , the amount of A quickly decreases while the amount of B increases rapidly, reaches a maximum at a shorter time, and then falls off with time.

Plasma concentration profile after intravenous administration of prodrug

Now consider a case for the intravenous administration of prodrugs (P) in which all the prodrugs are converted to active drugs (D) and then eliminated. In this case, the first-order formation rate constant for D, $k_{f(D)}$, is equal to the elimination

rate constant for P, $k_{el(P)}$. The parameter $k_{el(D)}$ represents the first order elimination rate constant for D. The rate of change of D in the blood is determined by the difference between the formation and the elimination rates. Because the level of each species in the blood is measured in concentration ($[D] = D/V_D$, where V_D is the volume of distribution for D), it is convenient to express Eq. (7) with the same unit. Then, using new notations ($k_1 \rightarrow k_{f(D)}$; $k_2 \rightarrow k_{el(D)}$), we get

$$[D] = \frac{k_{f(D)} V_P [P]_0}{V_D (k_{el(D)} - k_{f(D)})} (e^{-k_{f(D)} t} - e^{-k_{el(D)} t}) \quad (15)$$

where V_P is the volume of distribution for P, and $[P]_0$ is the initial concentration of P in the blood.

When plasma concentrations are measured as a function of time, the area under the concentration-time curve (AUC) is of great interest in pharmacokinetics. We can derive a useful relationship between AUC and clearance ($CL = k \times V$; volume/time in unit) by solving Eq. (2) using a concentration-time integral method. Writing Eq. (2) in new notations and taking the integral of both sides, we get

$$V_D \int_{[D]_0}^{\infty} d[D] = k_{el(P)} V_P \int_0^{\infty} [P] dt - k_{el(D)} V_D \int_0^{\infty} [D] dt. \quad (16)$$

Because D is not present in the body initially or at infinity, the left side becomes zero. Rearranging Eq. (16) and substituting $k_{el(P)} = CL_{(P)}/V_P$ and $k_{el(D)} = CL_{(D)}/V_D$, we get

$$\frac{AUC(D)}{AUC(P)} = \frac{k_{el(P)} V_P}{k_{el(D)} V_D} = \frac{CL_{(P)}}{CL_{(D)}} \quad (17)$$

This ratio is useful to study metabolic pathway and pharmacokinetic interactions.[8-10,13]

Elimination rate-limited (ERL) and formation rate-limited (FRL) metabolism

As shown in Eq. (15), the plasma drug concentration, $[D]$, at any given time is expressed by two exponential functions. Depending on the relationship between the prodrug and drug elimination rates, one term can become more dominant than the other. For a more detailed discussion, we consider two limiting situations. In the first situation, formation is a much faster process than elimination (ERL metabolism: $k_{f(D)} > k_{el(D)}$). In the second situation, formation proceeds much more slowly than elimination (FRL metabolism: $k_{f(D)} < k_{el(D)}$). To help understand the underlying kinetics, we simulated these situations to draw semi-logarithmic plots of plasma concentration versus time using Eq. (15) (Fig. 3).

In ERL metabolism, at large time, the first term approaches zero because $k_{f(D)} > k_{el(D)}$, and Eq. (15) reduces to

$$[D] = -\frac{k_{f(D)} V_P [P]_0}{V_D (k_{el(D)} - k_{f(D)})} e^{-k_{el(D)} t}. \quad (18)$$

Taking the logarithm to the base 10 of Eq. (18), we get

$$\log[D] = \log \left(\frac{k_{f(D)} V_P [P]_0}{V_D (k_{el(D)} - k_{f(D)})} \right) - \frac{k_{f(D)}}{2.303} t. \quad (19)$$

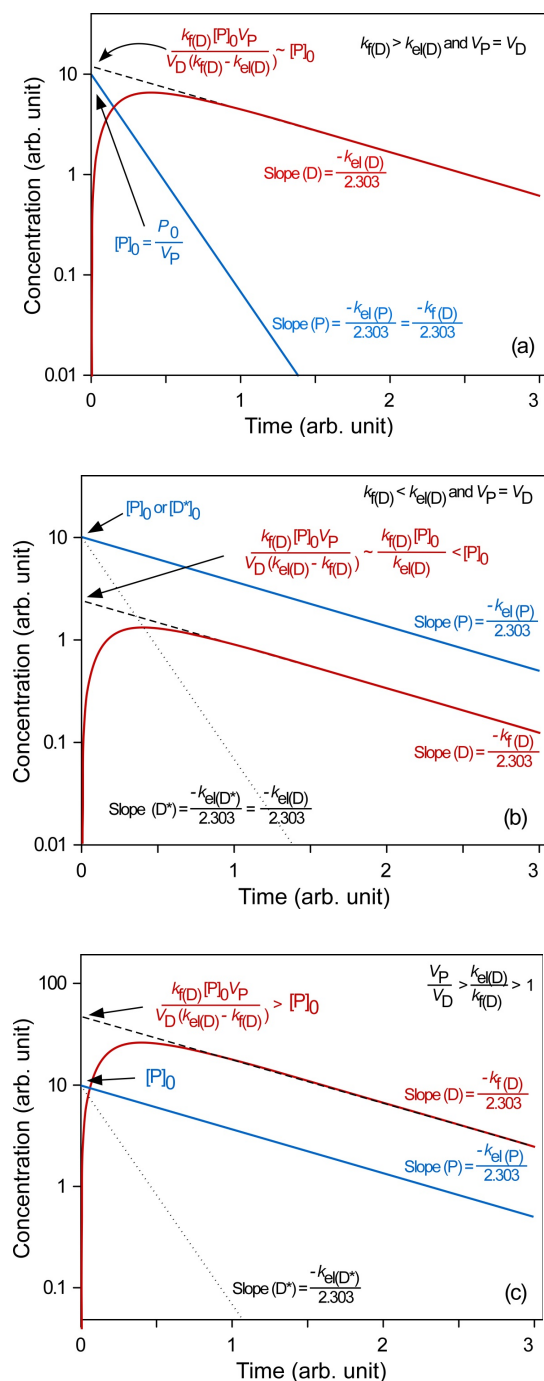


Figure 3. Semi-logarithmic concentration-time profile of a prodrug (P; blue line) and its formed metabolite (parent drug, D; red line). Simulations were performed using Microsoft Excel for three cases: (a) ERL metabolism where $k_{f(D)} > k_{el(D)}$: $k_{f(D)} = 5$, $k_{el(D)} = 1$, and $V_D = V_P = 1$, (b) FRL metabolism where $k_{f(D)} < k_{el(D)}$: $k_{f(D)} = 1$, $k_{el(D)} = 5$, and $V_D = V_P = 1$, and (c) FRL metabolism for $V_P/V_D > k_{el(D)}/k_{f(D)} > 1$: $k_{f(D)} = 1$, $k_{el(D)} = 5$, and $V_D = 0.05$, $V_P = 1$, and $A_0 = 10$. Back extrapolation (dashed line; plotted using Eq. (19) or (21)) of the elimination phase slope (red line) provides an estimate of $[D]_0$. The dotted line was plotted using Eq. (23) for the direct intravenous administration of a preformed (or synthesized) parent drug (D^*) with the initial amount of D^* (D^*_0) = 10 in (b) and 0.5 in (c). See text for details.

Thus, the semi-logarithmic plots of plasma concentration versus time become linear with a slope of $\frac{k_{el(D)}}{2.303}$ at large time. Back extrapolation (dashed line) of the elimination phase slope (red line) provides an estimate of $[D]_0$, which is the intercept of $\frac{k_{f(D)} V_P [P]_0}{V_D (k_{f(D)} - k_{el(D)})}$ (Fig. 3a). When $k_{f(D)} \gg k_{el(D)}$ and $V_P = V_D$, the intercept can be further reduced to $[P]_0$.

This situation is commonly encountered in the metabolism of many prodrugs.[10,15] An example is the metabolism of an antitrypanosomal compound (OSU-36) after an intravenous administration of its ester prodrug (OSU-40) to rat. The hydrolysis of OSU-40 was fast, and its concentrations declined rapidly with short half-life (4.8 min). Whereas, the concentrations of OSU-36, hydrolyzed from OSU-40, declined slowly with the half-life of 41.9 min. This was close to the elimination half-life of the preformed OSU-36 (43.9 min), directly administered to the systemic circulation by an intravenous injection.[15]

In FRL metabolism ($k_{f(D)} < k_{el(D)}$), at large time, Eq. (15) can be reduced in a similar way to give

$$[D] = \frac{k_{f(D)} V_P [P]_0}{V_D (k_{el(D)} - k_{f(D)})} e^{-k_{f(D)} t} \quad (20)$$

and

$$\log[D] = \log\left(\frac{k_{f(D)} V_P [P]_0}{V_D (k_{el(D)} - k_{f(D)})}\right) - \frac{k_{f(D)}}{2.303} t. \quad (21)$$

The slope and intercept of the semi-logarithmic plot of plasma concentration versus time are $\frac{k_{f(D)}}{2.303}$ and $\frac{k_{f(D)} V_P [P]_0}{V_D (k_{el(D)} - k_{f(D)})}$, respectively (Fig. 3b). In the elimination phase, thus, the concentration of the parent drug is governed by the prodrug formation rate, not by the prodrug elimination rate. Since $k_{f(D)} < k_{el(D)}$, the intercept can be further reduced to

$$\frac{k_{f(D)} V_P [P]_0}{V_D (k_{el(D)} - k_{f(D)})} \approx \frac{k_{f(D)} V_P}{k_{el(D)} V_D} [P]_0 = \frac{CL(P)}{CL(D)} [P]_0. \quad (22)$$

The plasma prodrug concentration, $[P]$, at any given time is easily obtained from Eq. (4), and its final semi-logarithmic expression is

$$\log[P] = \log([P]_0) - \frac{k_{el(D)}}{2.303} t. \quad (23)$$

In equations (21) and (23), it is worthwhile to note that the slopes are the same, that is, the concentrations of the parent drug and prodrug decline in parallel (Fig. 3b). Because the parent drug is eliminated almost as soon as it is formed, the elimination rate is approximately equal to the formation rate. The above equation can also be used to plot the plasma concentration-time profile of a preformed D (D^*) directly administered to the systemic circulation by an intravenous injection (dotted line). From Figure 3b, we can easily figure out that the half-life of the formed parent drug ($\ln 2/k_{f(D)}$) in the elimination phase is longer than that of the preformed parent drug ($\ln 2/k_{el(D)}$). The half-life of the formed parent drug reflects that of the prodrug ($\ln 2/k_{f(D)} = \ln 2/k_{f(D)}$).

The FRL metabolism is less encountered in prodrug kinetics but occasionally in metabolite kinetics.[10,13,16] One interesting example is the metabolism of 3'-azido-2',3'-dideoxy-5'-O-oxalatylthymidine (AZT-Ac) to zidovudine, [3'-azido-2',3'-dideoxythymidine (AZT)].[16] Only AZT was detected in

plasma, indicating that the prodrug is rapidly hydrolyzed in vivo with a high elimination rate constant. Thus, the first step looks like proceeding according to ERL-metabolism. However, the concentrations of AZT metabolized from AZT-Ac ($t_{1/2} = 2.16$ h) declined more slowly than those of AZT from preformed AZT ($t_{1/2} = 0.96$ h). This means that the metabolic pathway proceeds according to FRL metabolism ($k_{f(AZT)} < k_{el(AZT)}$), as discussed above. This discrepancy may be explained by the presence of multiple pathways for AZT-Ac elimination (small f in Fig. 1) or by the presence of another intermediate between AZT-Ac and AZT. Because AUC for AZT metabolized from AZT-Ac is slightly larger than that for AZT from preformed AZT at the same intravenous dose, the latter explanation looks more plausible.

In FRL metabolism, it is interesting to consider one more situation where $V_p/V_D > k_{el(D)}/k_{f(D)} > 1$, or $CL_{(p)} > CL_{(D)}$. As shown in Figure 3c, the intercept for the parent drug ($[D]_0$) is greater than that for the prodrug ($[P]_0$). This situation is encountered in the metabolic conversion of propranolol to naphthoxylactic acid (NLA) after single intravenous and oral doses.[17] The AUC of NLA was two times greater than that of propranolol after an intravenous dose of propranolol (4 mg) and ten times after a single oral dose (20 or 80 mg). This can be easily explained if the volume of distribution of NLA is much smaller than that of propranolol. The volumes of distribution of basic drugs are often larger than 100 L, while those of their acidic metabolites are close to 10~20 L.[13] Thus, this situation is expected to be common when a basic prodrug is converted to an acidic parent drug.

We described the prodrug kinetics for the simplest situation: formation and sequential elimination. We can consider a more complicated model to account for more realistic situations but will lose simplicity by including more terms in equations. A more detailed discussion is beyond the scope of this tutorial. For further study, we recommend to read articles and book chapters in the References section.

Acknowledgements

This study was supported by a grant of the Korean Health Technology R&D Project, Ministry of Health & Welfare, Republic of Korea (HI14C2750).

Conflicts of interests

- Authors: The authors have no conflicts of interest to declare.
- Reviewers: Nothing to declare
- Editors: Nothing to declare

References

1. Rautio J, Kumpulainen H, Heimbach T, Oliyai R, Oh D, Järvinen T, et al. Prodrugs: design and clinical applications. *Nat Rev Drug Discov* 2008;7:255-270. doi: 10.1038/nrd2468.
2. Zawilska JB, Wojcieszak J, Olejniczak AB. Prodrugs: a challenge for the drug development. *Pharmacol Rep* 2013;65:1-14.
3. Obach RS. Pharmacologically active drug metabolites: impact on drug discovery and pharmacotherapy. *Pharmacol Rev* 2013;65:578-640. doi: 10.1124/pr.111.005439.
4. Cummings AJ, Martin BK. Excretion and the accrual of drug metabolites. *Nature* 1963;200:1296-1297.
5. Martin BK. Kinetic considerations relating to the use of drug precursors. *Br J Pharmacol Chemother* 1967;31:420-434.
6. Houston JB. Drug metabolite kinetics. *Pharmacol Ther* 1982;15:521-552.
7. Houston JB, Taylor G. Drug metabolite concentration-time profiles: influence of route of drug administration. *Br J Clin Pharmacol* 1984;17:385-394.
8. Pang KS. A review of metabolite kinetics. *J Pharmacokinet Biopharm* 1985;13:633-662.
9. Smith PC. Pharmacokinetics of drug metabolites. In: Pearson PG, Wienkers LC (Eds.) *Handbook of drug metabolism*, 2nd ed. Informa Healthcare, New York, 2009;17-59.
10. de Campos ML, Padilha EC, Peccinini RG. A review of pharmacokinetic parameters of metabolites and prodrugs. *Drug Metab Lett* 2014;7:105-116.
11. Yang QJ, Pang KS. PBPK modeling to estimate metabolite formation from first-pass organs: intestine and liver. In: Chackalamannil S, Rotella D, Ward S. (Eds.) *Comprehensive medicinal chemistry III*, Volume 4, Elsevier, Oxford, 2017;83-101.
12. Sun H, Pang KS. Disparity in intestine disposition between formed and preformed metabolites and implications: a theoretical study. *Drug Metab Dispos* 2009;37:187-202. doi: 10.1124/dmd.108.022483.
13. Rowland M, Tozer TN. *Clinical pharmacokinetics and pharmacodynamics: concepts and applications*, 4th ed. Wolters Kluwer Health/Lippincott Williams & Wilkins, Philadelphia, 2011;603-632.
14. Atkinson AJ, Huang S-M, Lertora JLL, Markey SP. (Eds.) *Principles of Clinical Pharmacology*, 3rd ed. Academic Press, Amsterdam, 2012; 41-55.
15. Gershkovich P, Wasan KM, Sivak O, Lysakowski S, Reid C, Premalatha K, et al. Simultaneous determination of a novel antitrypanosomal compound (OSU-36) and its ester derivative (OSU-40) in plasma by HPLC: application to first pharmacokinetic study in rats. *J Pharm Pharm Sci* 2011;14:36-45.
16. Quevedo MA, Briñón MC. In vitro and in vivo pharmacokinetic characterization of two novel prodrugs of zidovudine. *Antiviral Res* 2009;83:103-111. doi: 10.1016/j.antiviral.2009.03.010.
17. Walle T, Conradi EC, Walle UK, Fagan TC, Gaffney TE. Naphthoxylactic acid after single and long-term doses of propranolol. *Clin Pharmacol Ther* 1979;26:548-554.